J Low Temp Phys (2014) 177:59–71
DOI 10.1007/s10909-014-1192-7

Ground State and Excitation Properties of Soft-Core Bosons

Tommaso Macrì · Sebastiano Saccani · Fabio Cinti

Received: 17 February 2014 / Accepted: 23 April 2014 / Published online: 9 May 2014

Abstract We study the physics of soft-core bosons at zero temperature in two dimensions for a class of potentials that could be realised in experiments with Rydberg dressed Bose-Einstein condensates. We analyze the ground state properties of the system in detail and provide a complete description of the excitation spectra in both superfluid, supersolid and crystalline phase for a wide range of interaction strengths and densities. In addition we describe a method to extract the transverse gapless excitation modes in the phases with broken translational symmetry within the framework of path integral Monte Carlo methods.

T. Macrì (✉)
Max Planck Institute for the Physics of Complex Systems, Nöthnitzer Straße 38,
01187 Dresden, Germany
e-mail: tommasomacri@gmail.com

T. Macrì
Max-Planck-Institut für Quantenoptik, Hans-Kopfermann-Str. 1, 85748 Garching, Germany

Present Address:
T. Macrì
QSTAR, Largo Enrico Fermi 2, 50125 Firenze, Italy
e-mail: macri@cqstar.eu

S. Saccani
SISSA Scuola Internazionale Superiore di Studi Avanzati and DEMOCRITOS National Simulation Center, Istituto Officina dei Materiali del CNR, Via Bonomea 265, 34136 Trieste, Italy
e-mail: sebastiano.saccani@gmail.com

F. Cinti
National Institute for Theoretical Physics (NITheP), Stellenbosch 7600, South Africa
e-mail: cinti@sun.ac.za

F. Cinti
Institute of Theoretical Physics, University of Stellenbosch, Stellenbosch 7600, South Africa

Keywords Soft-core bosons · Rydberg atoms · Elementary excitations · Path integral Quantum Monte Carlo

1 Introduction

A considerable number of theoretical studies have been lately devoted to investigate ultra-cold gases characterised by non-local interactions [1], such as dipolar bosons and fermions [2], Rydberg atoms [3], and polar molecules [4]. From the experimental perspective this field of research is increasingly turning into a perfect playground for realizing exotic phases with non-trivial broken symmetries [5–7], which are hardly observable in typical condensed matter systems. A primary example is the so called supersolid phase. Over the past few decades the existence of supersolidity was subjected to an extensive experimental and theoretical work, mostly dominated by studies on solid ^{4}He [8–15]. From a theoretical viewpoint supersolidity can be understood as a phase which simultaneously breaks both translational symmetry (crystalline order) and global gauge symmetry that enables long-range phase coherence and thereby superfluidity of the system [8]. Some recent theoretical investigations [16,17] proposed that a supersolid phase may emerge from a Bose-Einstein condensate where particles are off-resonantly excited to a Rydberg state. Under such conditions one can engineer effective two-body soft-core potentials which at large distances decay with the usual dipolar or Van der Waals power law, while at shorter ones approach a constant finite value—in contrast to the usual pure long range interactions– as a consequence of the dipole blockade effect [18]. Recently, quantum Monte Carlo (QMC) calculations in continuum space provided a complete description of the ground state phase diagram for soft-core bosons, confirming the presence of a cluster supersolid phase in two [19] and three dimensions [20]. Such superfluid clusters of a sufficient amount of particles per single site (high density regime) display physical properties which are also efficiently described by mean field approaches based on the solution of an effective non local Gross–Pitaevskii equation [20–22].

Lately, Cinti et al. [23] investigated the ground state features of soft-core bosons at lower densities where correlations can still give rise to supersolidity with a lower cluster occupancy. Interestingly, contrarily to the predictions of the mean field theory, at low densities superfluidity increases linearly with the number of zero-point defects in the ground state. This picture is indeed fully consistent with the mechanism proposed long ago by Andreev, Lifshitz [9] and Chester [10] (ALC), where superfluidity may, in fact, emerge through the formation of delocalized defects in the crystalline ground state.

The presence of two different microscopic mechanisms underlying the same macroscopic effect in different regimes of the parameter space, opens up other intriguing questions regarding static and dynamical properties of a supersolid. Recently it was shown for instance that the excitation spectrum of the supersolid displays well defined Goldstone modes [22,24], which emerge as a result of global gauge and translational symmetry breaking, respectively. It is not clear however how those modes show up and possibly deviate from the mean field approximation in the low density limit where correlations in the ALC regime are expected to be significant.

In the present paper we shall compare mean field results in the high and low density regime for a wide range of interaction strengths with exact QMC calculations for interaction potentials which can be simulated with Rydberg dressed atoms. Moreover we extend previous results concerning the spectrum of the elementary excitations extracting the transverse modes in the supersolid and crystalline phase with a method that exploits the crystalline arrangement of the ground state wavefunction. These calculations turn out to be essential to capture the range of validity of mean field calculations not only in the low density regime, but also at larger filling of the crystalline lattice where optical modes systematically shifts upwards the energy of the longitudinal mode in a way that is not controllable with advanced techniques of inversion of the intermediate scattering function [25].

The paper is organized as follow: In the next Section, after having introduced the system Hamiltonian, we discuss (Sect. 2.1) the mean-field approach based the Gross-Pitaevskii equation with a non-local Rydberg-dressed potential and define the Bogoliubov-de Gennes equations to study the excitation spectrum. QMC techniques are exposed in Sect. 2.2, focusing the attention on the method we employed to calculate the transverse excitations in the solid-like phase. In Sect. 3 we show the results regarding the ground state properties across the liquid–solid transition (Sect. 3.1), including a detailed analysis of the effects due to fluctuations in the uniform phase at high densities. In Sect. 3.2 we show the excitation spectra in the limit of high and low densities. In Sect. 4 we draw the conclusions and examine future extensions of the present work.

2 Physical System and Methodologies

We consider a system of bosons in two dimensions at zero temperature with mass m and positions $\mathbf{q}_i$, described by the Hamiltonian

$$\hat{H} = \sum_i -\frac{\hbar^2}{2m}\nabla_i^2 + \sum_{i<j} V(\mathbf{q}_i - \mathbf{q}_j). \tag{1}$$

The interaction is of soft-core nature and reads explicitly as $V(\mathbf{r}) = \frac{U}{r^6+R_c^6}$, being U and R_c strength and range of the interaction potential, respectively . For large inter-particle distances this potential shows a Van Der Waals-like power law decay, whereas for vanishing separation particles acquire a finite interaction energy U/R_c^6. Upon scaling lengths by R_c and energies by $\hbar^2/mR_c^2$, the zero temperature physics, determined by Eq. (1), depends only on two dimensionless parameters: an effective interaction strength $\alpha' = Um/\left(\hbar^2 R_c^4\right)$ and the dimensionless density $n\,R_c^2$.

2.1 Mean-Field Approach

Here we first review the mean field description [16,26] and the phases emerging from Eq. (1) at zero temperature [23]. In mean field theory the system dynamics is described by a non-local Gross-Pitaevskii equation (GPE), which reads in reduced units:

$$i\,\partial_t \psi(\mathbf{r},t) = \left(-\frac{\nabla^2}{2} + \alpha \int d\mathbf{r}' U(\mathbf{r}-\mathbf{r}')|\psi(\mathbf{r}',t)|^2\right)\psi(\mathbf{r},t)\ , \tag{2}$$

where $\mathbf{r} = \mathbf{q}/R_c$, $U(\mathbf{r}) = \frac{1}{1+r^6}$, and $\alpha = \alpha' n\, R_c^2 = m\, n\, U/\left(\hbar^2 R_c^2\right)$ is a dimensionless interaction strength that determines the ground state properties and the excitation dynamics. The energy associated to the state described by the wave function $\psi(\mathbf{r},t) = e^{-i\mu t}\psi_0(\mathbf{r})$ in Eq. (2) can be derived from the GP energy functional:

$$H = \int d\mathbf{r}\ \frac{1}{2}\,|\nabla\psi_0(\mathbf{r})|^2 + \frac{\alpha}{2}\int d\mathbf{r}\, d\mathbf{r}'\ |\psi_0(\mathbf{r})|^2 U(\mathbf{r}-\mathbf{r}')|\psi_0(\mathbf{r}')|^2\ . \tag{3}$$

In order to numerically determine the location of the transition from a uniform to a modulated ground state, we first expand the wavefunction $\psi_0(\mathbf{r})$ in Fourier series:

$$\psi_0(\mathbf{r}) = \sum_{\mathbf{Q}} C_{\mathbf{Q}}\, e^{i\,\mathbf{Q}\cdot\mathbf{r}}, \tag{4}$$

where $\mathbf{Q} = n\,\mathbf{b}_1 + m\,\mathbf{b}_2$ with n, m integers and $\mathbf{b}_1 = \frac{2\pi}{a}\left(1, -\frac{1}{\sqrt{3}}\right)$, $\mathbf{b}_2 = \frac{2\pi}{a}\left(0, \frac{2}{\sqrt{3}}\right)$ are the reciprocal lattice basis vectors of a triangular lattice. We then substitute Eq. (4) into Eq. (2) and iteratively solve the non-linear equations for $C_{\mathbf{Q}}$ until convergence is reached [27]. This procedure allows to determine the optimal lattice spacing, the chemical potential and the coefficients $C_{\mathbf{Q}}$.

The validity of the above mean field theory is limited to the regime of high densities, that is, where the depletion of the condensate remains small for a wide range of interaction strengths. Similar considerations were recently done on analogous soft-core step-like potentials leading to results in very good agreement with QMC simulations [22]. A through analysis of the ground state phase diagram for soft-core interactions as in Eq. (1) was provided in Ref. [23] both for the high and low density limit using QMC techniques and a schematic of the phase diagram is reported in Fig. 1, which are reviewed in Sect. 2.2.

In the high-density limit (when $n R_c^2 \gtrsim 1.8$) for low interaction strengths ($\alpha < 28$) the ground state of the system is in a uniform superfluid phase. Upon increasing the interaction at $\alpha \approx 28$ one crosses a first-order phase transition to a cluster supersolid phase characterized by a finite superfluid fraction and broken translational invariance where particles arrange in clusters (each cluster contains an average number of particles according to the density) in a triangular geometry. For even larger interactions $\alpha > 38$ the ground state preserves triangular symmetry but superfluidity vanishes resulting into an uncorrelated cluster crystal.

In the intermediate density regime ($0.5 \lesssim n R_c^2 \lesssim 1.8$) one observes a direct superfuid to crystal transition at commensurate lattice occupations where superfluidity vanishes abruptly. Simultaneously for incommensurate occupations of the crystalline lattice and mean field interactions in the range $28 < \alpha < 38$, superfluidity increases linearly with the fraction of vacancies or defects [23] in nice agreement with the ALC scenario of defect delocalization.

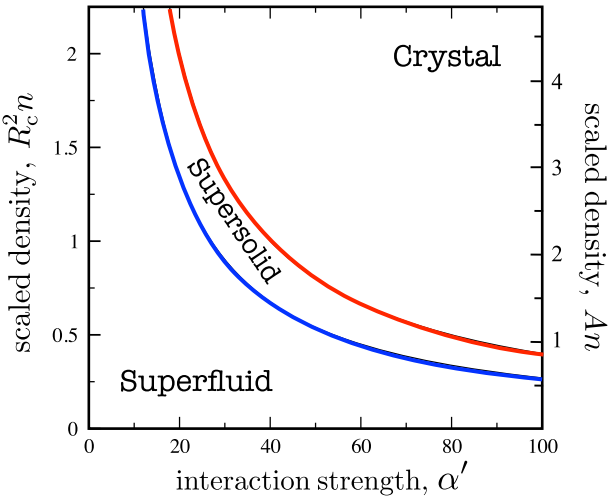

Fig. 1 Schematic phase diagram for the dimensionless parameters α' and the rescaled density nR_c^2. On the *right axis* we also show the average filling of the clusters in terms of the density An where $A = \frac{\sqrt{3}}{2}a^2$ is the area of the unit cell. The *hyperbolas mark* the superfluid–supersolid transition ($\alpha' nR_c^2 = 28$, *blue line*) and supersolid–crystal transition ($\alpha' nR_c^2 = 38$, *red line*) (Color figure online)

In the very low density limit ($nR_c^2 \lesssim 0.5$) the physics of the system becomes largely irrelevant of the detailed form of the soft core at small distances since the interparticle distance is much higher than the range of the potential. Indeed, upon increasing the interaction at fixed density the system displays a first order phase transition from a superfluid to a crystalline phase as expected for a standard Van der Waals interaction.

The elementary excitations in the mean field approximation are found by expanding the GP energy functional around the solution $\psi_0(\mathbf{r})$, obtaining the so called Bogoliubov de Gennes equations. Denoting the change in $\psi(\mathbf{r},t)$ by $\delta\psi(\mathbf{r},t) = e^{-i\mu t}\left[u(\mathbf{r})e^{-i\omega t} - v^*(\mathbf{r})e^{i\omega t}\right]$ and substituting this expression into the GPE Eq. (2) we find a set of two coupled linear differential equations:

$$\begin{cases} \left(-\frac{\nabla^2}{2} - \mu - \omega\right) u(\mathbf{r}) + \alpha \int d\mathbf{r}' U(\mathbf{r}-\mathbf{r}') \left[\psi_0(\mathbf{r}')^2 u(\mathbf{r}) + \psi_0(\mathbf{r})\psi_0(\mathbf{r}') \left(u(\mathbf{r}') - v(\mathbf{r}')\right)\right] = 0 \\ \left(-\frac{\nabla^2}{2} - \mu + \omega\right) v(\mathbf{r}) + \alpha \int d\mathbf{r}' U(\mathbf{r}-\mathbf{r}') \left[\psi_0(\mathbf{r}')^2 v(\mathbf{r}) - \psi_0(\mathbf{r})\psi_0(\mathbf{r}') \left(u(\mathbf{r}') - v(\mathbf{r}')\right)\right] = 0 \end{cases} \tag{5}$$

for the Bogoliubov amplitudes $u(\mathbf{r})$ and $v(\mathbf{r})$. The solution of Bogoliubov Eqs.(5) in the uniform superfluid phase is analytical:

$$\epsilon_q = \sqrt{\frac{q^2}{2}\left(\frac{q^2}{2} + 2\alpha\,\tilde{U}_q\right)}, \tag{6}$$

and depends only on the modulus of the excitation vector $\mathbf{q}$. Here $\tilde{U}_q$ is the Fourier transform of the potential (see Eq. (13) for an expression in terms of special functions). The spectrum is linear for small momenta and the slope defines the sound velocity of

the system; for $\alpha \geq 5.4$ one recovers the usual roton-maxon spectrum that is common to other physical systems with non-local interactions as ultracold dipolar systems or superfluid ^{4}He. In nonuniform phases one has to rely on a numerical solution of Eq. (5). Ref.[27] uses for example a Fourier expansion of the Bogoliubov amplitudes followed by a diagonalization of the corresponding equations. The results that we present in Sec.(3.2) are instead obtained using a grid based solution in real space of the Eqs.(5) for the lowest excitation bands and for $\mathbf{q}$ vectors lying in the first Brillouin zone (FBZ) [22] .

2.2 Monte Carlo Approach

In order to assess the validity of mean field theory and extend these results to the regime of lower densities we performed QMC calculations [28] at finite temperature based on the worm algorithm [29,30] in the canonical ensemble, carefully extrapolating the zero temperature limit. We do not enter here into a detailed description of the algorithm to measure thermodynamic observables (the reader can refer to Ref. [30] for an extensive summary of such techniques). Here we focus on the application of QMC to recover information about the spectrum of the elementary excitations of the system under study. In particular, it is possible to sample directly the imaginary-time intermediate scattering function

$$F(\mathbf{k}, \tau) = \langle \hat{\rho}_{\mathbf{k}}(\tau) \hat{\rho}^{\dagger}_{\mathbf{k}}(0) \rangle / N, \tag{7}$$

where the brackets denote a thermal average and

$$\hat{\rho}_{\mathbf{k}} = \sum_j e^{i\mathbf{k}\cdot\mathbf{q}_j} \tag{8}$$

is the density fluctuation operator at wavevector $\mathbf{k}$. The dynamic structure factor $S(\mathbf{k}, \omega)$, which contains the information on the spectrum of the elementary excitations of the density fluctuations, is related to $F(\mathbf{k}, \tau)$ via an inverse Laplace transform:

$$F(\mathbf{k}, \tau) = \int \mathrm{d}\omega \, e^{-\tau\omega} S(\mathbf{k}, \omega). \tag{9}$$

Here we face the well known ill-defined problem of inverting the Laplace transform from noisy data. There exists no general scheme to recover the exact inversion, however some techniques manage to identify weight and frequency of the dominant contributions of a spectrum composed of well-defined peaks [25,31]. However, previous investigations on bosonic systems with soft-core bosons with a step interaction potential [24] showed that fitting the $F(\mathbf{k}, \tau)$ data directly via an n-pole approximation, i.e. assuming that the spectrum $S(\mathbf{k}, \omega)$ is formed by a sum of n delta functions of ω gives equally reliable results in good quantitative agreement with more involved techniques based on the genetic inversion via falsification of the theories (GIFT) approach [25]. For such reasons in this work we focus on the n-pole approximation results to extract the excitation spectrum.

The estimator defined in Eq. (7) within the FBZ only contains information about longitudinal density fluctuations. A study of the longitudinal modes was done for a class of soft-core potentials in [24]. The extension to the transverse excitations is not straightforward as it requires a careful analysis of the contributions to the intermediate scattering function outside the FBZ. However, the spectral weight outside the FBZ is generically distributed on a greater number of modes, making difficult to perform the analytic continuation of the Laplace transform, as excitations near in energy tend to merge in the reconstructed spectra.

In order to obtain the dispersion relation for transverse modes, one may measure imaginary-time current correlations [32] and then perform the inverse Laplace transform. However, these current correlations estimators generically display much larger statistical errors than simple density correlations, making the analytical continuation unfeasible in most cases.

Although it is possible to derive such current estimators with a reduced statistical error within a method described in [33], we use here a different and numerically less demanding strategy to couple transverse excitations in a lattice system to density fluctuations inside the FBZ. The idea behind our method is to alter the imaginary time particle positions while applying the density fluctuation operator so that transverse lattice displacements mimic longitudinal displacements, and vice-versa. For each slice in imaginary time we first identify the positions of the lattice sites of a triangular lattice to which particles belong (the nearest one). We then apply a weak potential to avoid the slow translations and rotations of the lattice as a whole that may occur in the simulations, so that their positions remain fixed. This potential is two orders of magnitude weaker than the average one between two lattice sites, so it does not alter the dispersion relations significantly. For each time slice and particle position, we identify the nearest lattice site and rotate the particle position by $\pi/2$ with respect to it. With this modified configuration we compute the density fluctuation operator defined in Eq. (8) and from then on we follow the same procedure as in the standard case for obtaining excitation energies via Eq. (7) and the n-pole approximation.

The above operation transforms transverse lattice displacements so that they resemble longitudinal excitations. To show this, we first write the j particle position as $\mathbf{q}_j = \mathbf{R}_j + \delta\mathbf{q}_j$, where $\mathbf{R}_j$ is the position of the closest lattice site to the particle labeled by index j and $\delta\mathbf{q}_j$ is the relative displacement vector to the lattice site $\mathbf{R}_j$.

Then we perform a local rotation of the relative displacement $\delta\mathbf{q}_j$ by $\pi/2$ with respect to the corresponding lattice site $\mathbf{R}_j$ applying a rotation matrix:

$$M_{\pi/2} = \begin{pmatrix} 0 & -1 \\ 1 & 0 \end{pmatrix}, \tag{10}$$

and then calculate again the density operator:

$$\hat{\rho}'_{\mathbf{k}} = \sum_j e^{i\mathbf{k}\cdot(\mathbf{R}_j + (M_{\pi/2}\,\delta\mathbf{q}_j))} = \sum_j e^{i(M^T_{\pi/2}\,\mathbf{k})\cdot((M^T_{\pi/2}\,\mathbf{R}_j)+\delta\mathbf{q}_j)}, \tag{11}$$

where the last term follows from the properties of the scalar product. Because of the presence of a rotation matrix, the term $M^T_{\pi/2}\,\mathbf{k}\cdot\delta\mathbf{q}_j$ is proportional to the component

of $\delta\mathbf{q}_j$ orthogonal to $\mathbf{k}$, while of course in the absence of any rotation it would be proportional the the component of $\delta\mathbf{q}_j$ parallel to $\mathbf{k}$. Transverse excitations are therefore recorded in the transformed density fluctuation operator $\hat{\rho}'_{\mathbf{k}}$ even if $\mathbf{k}$ lies within the FBZ.

As expected, the present reasoning is based on the assumption that the crystalline structure exists and that we can unambiguously identify for each particle the lattice site to which it is pertaining. It is worth stressing that the configuration produced by the transformation defined above is merely a trick used to couple a term like the one in Eq. (8) to transverse excitations and leaves unaffected the internal Monte Carlo dynamics.

3 Results

3.1 Ground States Properties

In the upper panel of Fig. 2 we report the mean field energy per particle of the uniform phase $e_{uni} = 2\pi^2/3\sqrt{3}$ otained with full numerical minimization of Eq. (3). For $\alpha < \alpha_{c,MF} = 26.6$ the density is homogeneous and the system is then superfluid; upon increasing the interaction one crosses a first order phase transition to a phase with a modulated density. In the lower panel (again Fig. 2) we show the kinetic energy per particle comparing QMC results extrapolated to the $T \to 0$ limit, and the values from mean field. QMC data clearly display an abrupt jump of the kinetic energy for

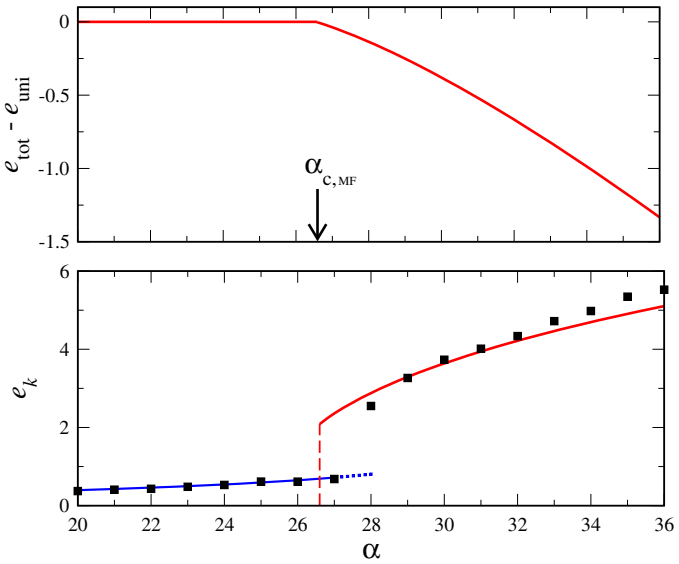

Fig. 2 *Upper panel* Energy difference between the uniform state and the modulated state in the mean field approach obtained by minimizing the Gross–Pitaevskii energy functional in Eq. (3). The SF-SS transition is located at $\alpha = 26.6$ for the value of lattice spacing equal to $a/R_c = 1.6$. *Lower panel* kinetic energy per particle from QMC calculations for 400 particles at density $nR_c^2 = 4.5$. The red line is the kinetic term of Eq. (3). In this approximation in the uniform phase kinetic energy vanishes. The *blue line* is a beyond mean field calculation of the kinetic energy based on Eq. (12) for density $n\,R_c^2 = 4.5$ that well agrees with QMC data. *Error bars* on QMC data are smaller than the dimension of the points (Color figure online)

$27 < \alpha < 28$ signaling the transition to the supersolid phase in good agreement with the mean field results within few percents.

We also included Bogoliubov fluctuations energy on top of the uniform solution that is displayed as the solid line from $\alpha = 20$ to $\alpha \approx 27$ in Fig. 2 (lower panel). This calculation is based on the evaluation of the following integral [34]:

$$e_{kin} = \frac{1}{8\pi n} \int_0^\infty dq\, q^3 \left(\frac{\frac{q^2}{2} + \alpha\, \tilde{U}_q}{\sqrt{\frac{q^2}{2}\left(\frac{q^2}{2} + 2\alpha\, \tilde{U}_q\right)}} - 1 \right), \tag{12}$$

where $\tilde{U}_q$ is the Fourier transform of the interaction potential:

$$\tilde{U}_q = \frac{\pi}{3} \mathbf{G}_{0,6}^{4,0}\left(\frac{q^6}{46656} \middle| 0\ \tfrac{1}{3}\ \tfrac{2}{3}\ \tfrac{2}{3}\ 0\ \tfrac{1}{3} \right) \tag{13}$$

and $\mathbf{G}_{p,q}^{m,n}\left(z \middle| \begin{matrix} a_1, \ldots, a_p \\ b_1, \ldots, b_q \end{matrix} \right)$ is the Meijer's G-function [35].

We see that Eq. (12) matches very well the QMC calculations performed in the superfluid phase. These results can be understood noting that the condensate fraction is relatively high for this class of soft-core potentials when the density is sufficiently high [22,36,37]. In order to verify this assertion, we calculated the depletion n_{exc}/n in the superfluid phase within the Bogoliubov approximation and obtained the largest value $n_{exc}/n \approx 38$ % close to the transition.

3.2 Excitations

In Fig. 3 we show the dispersion relations, ω_q versus $q\,R_c$, obtained applying the one-pole approximation (points, within QMC simulations, see Sect. 2.2), and the

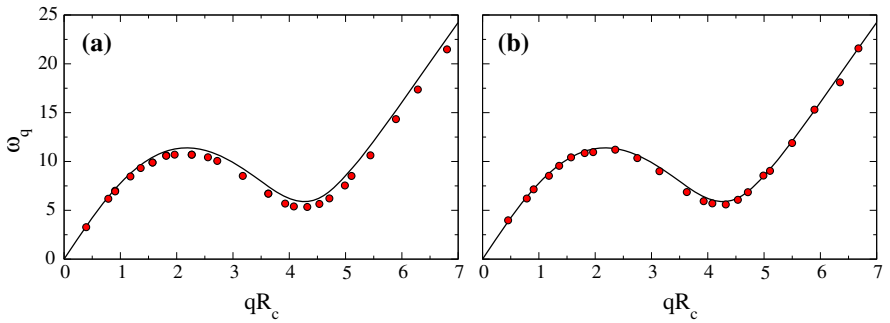

Fig. 3 Spectra in the superfluid phase at $\alpha = 20$ with the typical roton–maxon feature. *Dots* correspond to the one-pole approximations and are compared with the solution of Bogoliubov–de Gennes Eqs. (6) (*full line*). Excitation energy is in units of $\hbar^2/mR_c^2$. **a** Density $n\,R_c^2 = 1.12$. **b** $n\,R_c^2 = 3.8$. *Error bars* on the frequencies are recovered from the one-pole approximation and are smaller than the point size (Color figure online)

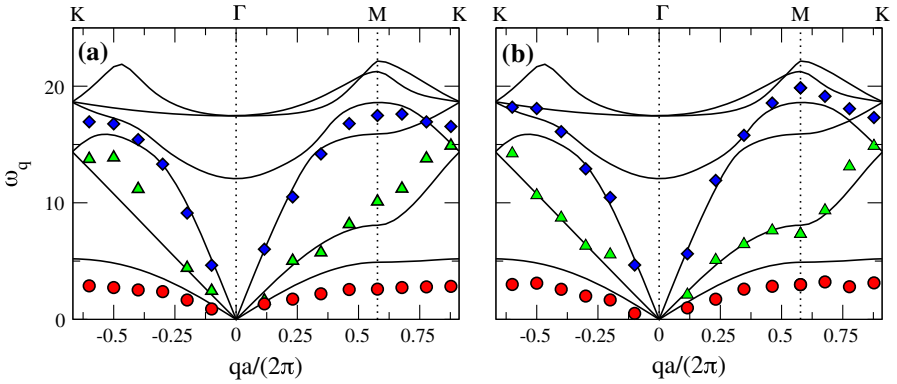

Fig. 4 Excitation spectra in the supersolid phase with an interaction strength $\alpha = 34$. *Dots* correspond to the n-pole approximations, *red circle* Bogoliubov band, *blue diamond* longitudinal modes, and *green triangle* transverse modes. They are compared with the numerical solution of Bogoliubov–de Gennes Eqs. (5) (*full lines*). Excitation energy is in units of $\hbar^2/mR_c^2$. **a** Density $nR_c^2 = 1.12$. **b** Density $nR_c^2 = 3.8$ (Color figure online)

analytical mean-field solution of Bogoliubov (see Eqs. (6), continuous lines) at low (Fig. 3a, $n\,R_c^2 = 1.12$) and high density (Fig. 3b, $n\,R_c^2 = 3.8$), respectively. Both panels present results at the same mean field interaction strength, $\alpha = 20$. Such an interaction turns out to be high enough for exhibiting an unambiguous roton instability. In Fig. 3a the simulations have been performed using 250 particles while at the higher density (Fig. 3b) we have used 850 particles. Mean-field calculations quantitatively agree with QMC simulations with a small deviation (about 5%) between the two approaches for the lowest density at higher momenta. We interpret this disagreement as an effect of the stronger correlations in the low density limit [23].

In Fig. 4, we plot the excitation spectra in the supersolid phase at mean field interaction $\alpha = 34$ with the same densities as in Fig. 3. Mean-field theory predicts three Goldstone modes that reflect the three spontaneously broken symmetries in a supersolid phase. The lowest band corresponds to the Bogoliubov mode that appears due to the off-diagonal long range order of the one body density matrix. The other two gapless bands are a consequence of the broken translational symmetry of the crystalline structure. Specifically, the highest gapless mode is a longitudinal band, whereas the intermediate mode is a transverse excitation [22].

At high filling (Fig. 4b) one can notice a satisfactory agreement between mean-field results and QMC spectra, in particular for the transverse band. Nevertheless, due to its limited resolution at higher energies, QMC does not allow to distinguish among longitudinal mode contributions and optical bands, since they are very close in energy for intermediate interactions. It is worth mentioning that, for both densities, mean-field theory predicts a larger Bogoliubov branch compared to QMC points. We mention that we have observed a similar behaviour in the entire supersolid regime. Finally, at lower densities the mean field theory still qualitatively agrees with QMC, even though the transverse band deviates systematically to larger energies if confronted to higher densities.

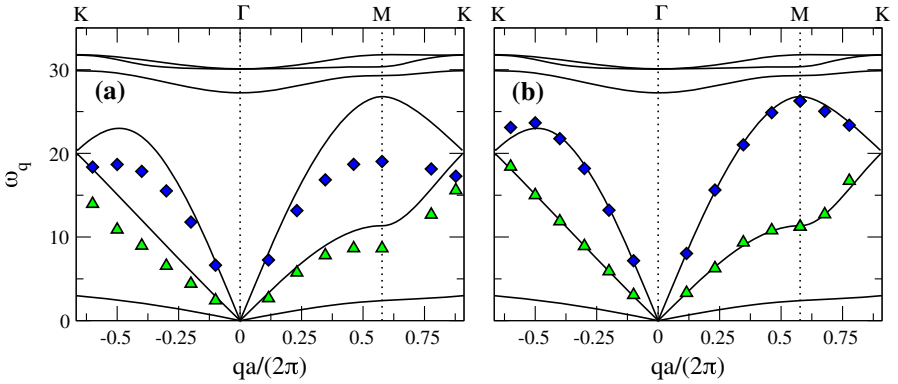

Fig. 5 Excitation spectra in the crystal phase with an interaction strength $\alpha = 60$. *Dots* correspond to the n-pole approximations, *blue diamond* longitudinal modes, and *green triangle* transverse modes. They are compared with the numerical solution of Bogoliubov–de Gennes Eqs. (5) (*full lines*). Excitation energy is in units of $\hbar^2/mR_c^2$. **a** Density $nR_c^2 = 1.12$. **b** Density $nR_c^2 = 3.8$ (Color figure online)

Now we discuss the excitation spectrum in the crystalline phase. QMC shows that for interactions $\alpha \gtrsim 38$ superfluidity vanishes as well as the contribution of the Bogoliubov band to the structure factor. Figure 5a, b report the energy of the elementary excitations at $\alpha = 60$, again for the same densities as in Fig. 3. We observe that the Bogoliubov mode is still present from mean field calculations due to the global coherency assumed in the derivation of Eqs. (5) even for very large interactions. Simultaneously at large densities gapless modes are far in energy from the optical branches. We indeed see that Fig. 5b provides a good matching between the prediction of longitudinal and transverse modes by QMC and the approach of Sect. 2.1. Finally, we observe that in Fig. 5a correlations limit the predictive power of the Bogoliubov equations that show deviations up to ≈ 30 % for large momenta.

4 Conclusion

In the present paper we analyzed in detail some significant properties of soft-core bosons interacting through a soft-core potential that can be realized with Rydberg-dressed atoms. In particular, we considered a two dimensional system at zero temperature, with an interaction range such that the ground state displays a supersolid phase. In particular, we extended some previous studies [22,24] by calculating the transverse gapless mode within a QMC approach. This technique allows to evaluate accurately the transverse excitations in a translationally broken phase, with statistical errors comparable to the ones obtained by the standard procedure used for longitudinal excitations [24].

In the regime of density-modulated superfluid, we have compared mean-field results with exact QMC calculations, verifying that the ground state and the elementary excitations are quantitatively described by a non-local Gross–Pitaevskii equation supplemented by the fluctuations encoded in the Bogoliubov formalism. Within this framework, we have included the Bogoliubov fluctuations and checked that the average

kinetic energy is fully consistent with the QMC calculations in the high density limit. Yet, a comparison between the numerical simulation based on the calculation of the intermediate scattering function and the solutions of the Bogoliubov–de Gennes equations in the supersolid phase reveals a convincing agreement, as previously observed for the longitudinal phonon and Bogoliubov modes in the case of a step-like interaction potential [22]. On the other hand the global phase coherence assumed in the mean field approach overestimates the energy of the Bogoliubov excitation band with respect to QMC calculations, both in the supersolid and in the crystalline phase and it can be as large as 30 % for large momenta.

Concerning the low density regime, i.e. where quantum fluctuations are expected to play a major role, we conclude that mean field computations still quantitatively predict the spectra for a uniform superfluid for a wide range of momenta and interactions. At the same time, for supersolid and crystalline phases the deviations from QMC become larger upon increasing the interactions, reaching approximately 30 % for an interaction strength $\alpha = 60$ and density $nR_c^2 = 1.12$.

The predictions made in this work may serve as a guidance for further theoretical and experimental studies on supersolidity with laser excited Bose–Einstein condensates. A natural extension of this work, for instance, might regard the behaviour of soft-core bosons in three dimensions in the low density regime to complement and extend recent analysis on cluster supersolidity [16,20,38] which would though require more refined techniques to calculate transverse modes in inhomogeneous phases. Finally we mention that the analysis of the spectrum could provide a natural way to observe supersolidity in the laboratory [39–41]. Several experimental techniques have indeed been recently tested and implemented in ultra-cold atomic systems to detect elementary excitations, including Bragg [42,43] and Raman spectroscopy [44].

Acknowledgments We acknowledge M. Boninsegni, G. Carleo, S. Moroni, and T. Pohl for valuable discussions.

References

1. I. Bloch, J. Dalibard, W. Zwerger, Rev. Mod. Phys. **80**, 885 (2008)
2. T. Lahaye, C. Menotti, L. Santos, M. Lewenstein, T. Pfau, Rep. Prog. Phys. **72**(12), 126401 (2009)
3. M. Saffman, T.G. Walker, K. Mølmer, Rev. Mod. Phys. **82**, 2313 (2010)
4. A. Micheli, G. Pupillo, H.P. Büchler, P. Zoller, Phys. Rev. A **76**(4), 043604 (2007)
5. M.A. Baranov, M. Dalmonte, G. Pupillo, P. Zoller, Chem. Rev. **112**(9), 5012 (2012)
6. G. Pupillo, A. Micheli, H.P. Büchler, P. Zoller, in *Cold Molecules: Creation and Applications*, ed. by R.V. Krems, B. Friedrich, W.C. Stwalley (Taylor and Francis, 2008)
7. P. Schauß, M. Cheneau, M. Endres, T. Fukuhara, S. Hild, A. Omran, T. Pohl, C. Gross, S. Kuhr, I. Bloch, Nature **491**(7422), 87 (2012)
8. M. Boninsegni, N.V. Prokof'ev, Rev. Mod. Phys. **84**, 759 (2012)
9. A.F. Andreev, I.M. Lifshitz, Sov. Phys. Jetp-USSR **29**(6), 1107 (1969)
10. G.V. Chester, Phys. Rev. A **2**(1), 256 (1970)
11. A.J. Leggett, Phys. Rev. Lett. **25**, 1543 (1970)
12. M.W. Meisel, Phys. B **178**(1–4), 121 (1992)
13. E. Kim, M.H.W. Chan, Nature **427**(6), 225 (2004)
14. E. Kim, M.H.W. Chan, Science **305**(6), 1941 (2004)
15. D.Y. Kim, M.H.W. Chan, Phys. Rev. Lett. **109**, 155301 (2012)
16. N. Henkel, R. Nath, T. Pohl, Phys. Rev. Lett. **104**(19), 195302 (2010)

17. G. Pupillo, A. Micheli, M. Boninsegni, I. Lesanovsky, P. Zoller, Phys. Rev. Lett. **104**(22), 223002 (2010)
18. M.D. Lukin, M. Fleischhauer, R. Cote, L.M. Duan, D. Jaksch, J.I. Cirac, P. Zoller, Phys. Rev. Lett. **87**, 037901 (2001)
19. F. Cinti, P. Jain, M. Boninsegni, A. Micheli, P. Zoller, G. Pupillo, Phys. Rev. Lett. **105**(13), 135301 (2010)
20. F. Ancilotto, M. Rossi, F. Toigo, Phys. Rev. A **88**, 033618 (2013)
21. Y. Pomeau, S. Rica, Phys. Rev. Lett. **72**(15), 2426 (1994)
22. T. Macrì, F. Maucher, F. Cinti, T. Pohl, Phys. Rev. A **87**, 061602 (2013)
23. F. Cinti, T. Macrì, W. Lechner, G. Pupillo, T. Pohl, Nat. Commun. **5**, 3235 (2014)
24. S. Saccani, S. Moroni, M. Boninsegni, Phys. Rev. Lett. **108**, 175301 (2012)
25. E. Vitali, M. Rossi, L. Reatto, D.E. Galli, Phys. Rev. B **82**, 174510 (2010)
26. Y. Pomeau, S. Rica, Phys. Rev. Lett. **72**, 2426 (1994)
27. M. Kunimi, Y. Kato, Phys. Rev. B **86**, 060510 (2012)
28. D.M. Ceperley, Rev. Mod. Phys. **67**(2), 279 (1995)
29. M. Boninsegni, N. Prokof'ev, B. Svistunov, Phys. Rev. Lett. **96**(7), 070601 (2006)
30. M. Boninsegni, N.V. Prokof'ev, B.V. Svistunov, Phys. Rev. E **74**(3), 036701 (2006)
31. M. Jarrell, J.E. Gubernatis, Phys. Rep. **269**(3), 133 (1996)
32. E.L. Pollock, D.M. Ceperley, Phys. Rev. B **36**, 8343 (1987)
33. G. Carleo, G. Boéris, M. Holzmann, L. Sanchez-Palencia, Phys. Rev. Lett. **111**, 050406 (2013)
34. C. Pethick, H. Smith, *Bose–Einstein Condensation in Dilute Gases* (Cambridge University Press, Cambridge, 2002)
35. I.S. Gradshteyn, I.M. Ryzhik, *Table of Integrals, Series, and Products*, 7th edn. (Elsevier/Academic Press, Amsterdam, 2007)
36. M. Schick, Phys. Rev. A **3**, 1067 (1971)
37. S. Pilati, J. Boronat, J. Casulleras, S. Giorgini, Phys. Rev. A **71**, 023605 (2005)
38. F. Maucher, N. Henkel, M. Saffman, W. Królikowski, S. Skupin, T. Pohl, Phys. Rev. Lett. **106**, 170401 (2011)
39. D.M. Stamper-Kurn, A.P. Chikkatur, A. Görlitz, S. Inouye, S. Gupta, D.E. Pritchard, W. Ketterle, Phys. Rev. Lett. **83**, 2876 (1999)
40. J. Steinhauer, R. Ozeri, N. Katz, N. Davidson, Phys. Rev. Lett. **88**, 120407 (2002)
41. D. Clément, N. Fabbri, L. Fallani, C. Fort, M. Inguscio, J. Temp. Phys. **158**(1–2), 5 (2010)
42. S.B. Papp, J.M. Pino, R.J. Wild, S. Ronen, C.E. Wieman, D.S. Jin, E.A. Cornell, Phys. Rev. Lett. **101**, 135301 (2008)
43. D. Clément, N. Fabbri, L. Fallani, C. Fort, M. Inguscio, Phys. Rev. Lett. **102**, 155301 (2009)
44. T.L. Dao, A. Georges, J. Dalibard, C. Salomon, I. Carusotto, Phys. Rev. Lett. **98**, 240402 (2007)